The small strain stiffness from bender elements tests for clayey soils

KATARZYNA MARKOWSKA-LECH[1], WOJCIECH SAS[1], MARIUSZ LECH[2], KATARZYNA GABRYŚ[1], ALOJZY SZYMAŃSKI[2]
[1] Water Center Laboratory, Faculty of Civil and Environmental Engineering, Warsaw University of Life Sciences – SGGW
[2] Faculty of Civil and Environmental Engineering, Warsaw University of Life Sciences – SGGW

Abstract: *The small strain stiffness from bender elements tests for clayey soils*. The shear modulus of soils at small strain (G_0) is one of the input parameters in a finite element analysis with the hardening soil model with small strain stiffness, required in the advanced numerical analyses of geotechnical engineering problems. The small strain stiffness can be determined based on the seismic wave velocities measured in the laboratory and field tests, but the interpretation of test results is still under discussion because of many different factors affecting the measurements of the wave travel time. The recommendations and proposed solutions found in the literature are helpful as a guide, but ought to be adopted with a certain measure of care and caution on a case-by-case basis. The equipment, procedures, tests results and interpretation analyses of bender elements (BE) tests performed on natural overconsolidated cohesive soils are presented.

Key words: small strain stiffness, bender elements, clays

INTRODUCTION

In recent years, there has been an increasing interest in describing the mechanical behaviour of soils at small strain. The shear modulus at very small strain G_0 (the initial shear modulus) is widely considered to be a fundamental property of the soil stiffness and is crucial in practical geotechnical solutions, particularly in the prediction of soil-structure interaction and earthquake engineering (Lo-Presti et al. 1999, Schneider et al. 1999, Pelli et al. 2004, Schinad 2005, Stokoe et al. 2005, Clayton 2011, Lipiński et al. 2017). Hardin and Black (1968) have identified the major factors contributing to the actual value of the shear modulus, such as vertical effective stress, void ratio, overconsolidation ratio (*OCR*), soil fabric, temperature and the degree of saturation.

The initial shear modulus (G_0) of the soil at induced strain levels less than 0.0001% can be obtained from the shear wave velocity using the following equation:

$$G_0 = \rho \cdot V_s{}^2 \tag{1}$$

where:
ρ – mass density;
V_s – shear waves velocity for linear, elastic and isotropic medium.

The most developed techniques, which are represented by a combination of standard geotechnical tests with geophysical test module (shear wave velocity measurements), have been used both in the laboratory and in the field tests. Field techniques include the seismic cone penetration test, the seismic flat dilatometer, the crosshole test and the SASW. Laboratory tests include resonant column, torsional shear and triaxial shear tests with local strain measurement and bender element test (Schneider et al. 1999, Schnaid 2005). Those configurations diminish the disadvantages of each test group and significantly enhance the optimization of data collection (Wolski and Lipiński 2006). In our paper the results of bender element test performed on natural cohesive soils are presented.

Various methods have been studied for determining the travel time such as the first arrival time, the travel time between the characteristic points, and the cross-correlation method (Viggiani and Atkinson 1995, Brignoli et al. 1996, Jovicic el al. 1996, Arulantan et al. 1998, Zeng and Ni 1999, Lee and Santamarina 2005, Leong at al. 2005, Yamashita et al. 2007, Chee-Ming 2012). As reported in the literature, there is still some uncertainty regarding the best method of shear wave arrival time definition, be it in the time or frequency. Although some other researchers have claimed that frequency domain methods are more reliable, visual picking of the arrival time in the time domain was found to be equally good, and had the advantage of being simpler and quicker (Chee-Ming 2012).

Nowadays, a bender element test is commonly used to measure the shear wave velocity in laboratory conditions. A piezoelectric bender element test is a relatively simple non-destructive test to measure shear and compression wave velocities and determine the shear modulus. But the number of different factors affecting the measurements of the travel time in the bender elements tests causes difficulties in choosing the reliable method of determination of the first arrival time and there is no standard method for this tests (Clayton 2011, Table 1).

TABLE 1. Variants in bender element testing (after Clayton 2011)

Issue	Brief description	Effect	Suggested standard
Bender dimensions	Width and protrusion into the specimen	Travel distance is generally accepted as bender tip-to-tip. Reduced travel distance causes reduced accuracy. Installation of highly protruding bender elements is more difficult in specimens of stiff/hard natural sediment	Most laboratories adopt 10 mm width, 0.5–1.0 mm thickness, and a protrusion of < 5 mm. Shorter protrusion (approx.1 mm) is favoured in the UK when testing stiff natural materials, where otherwise a slot needs to be cut and the bender filled around during installation. Fixing epoxy is set back inside end caps, and the space filled with silicone rubber compound, to allow flexing of the bender element

TABLE 1. cont.

Issue	Brief description	Effect	Suggested standard
Bender construction	Transmitter and receiver bender configurations, extender elements, and self-monitoring configurations	Using different (series and parallel) bimorphs as transmitter and receiver improves shear wave generation and reception. Extender elements allow P-wave generation. Use of a self-monitoring configuration, allows the movement of the bimorph (as distinct from its driving voltage) to be determined	Experience suggests that the wiring of benders as S-wave transmitters, P-wave transmitters and S-wave receivers gives advantages. Self-monitoring bender elements may be useful, as they allow the detection of time lags and phase changes between driving voltage and actual movement of the transmitter, resulting from characteristic impedance mismatch
Location of bender elements	Bender elements may be mounted in the rigid base and top caps of cells, or through the triaxial membrane	Mounting across or along specimens allows shorter travel distances (giving reduced attenuation and higher S/N ratio), and determination of the velocity of waves polarised in different directions. Very-small strain anisotropy of stiffness can then be inferred from shear wave velocities	The addition of side-mounted bender elements is relatively easy to achieve using grommets and O-rings similar to those for mid-plane pore water pressure measurement
Travel distance	Small tip-to-tip travel distance affects travel time resolution. Large distance increases attenuation	Closely spaced benders display more scatter in calculated shear wave velocity. Data from widely spaced benders are more noisy. The estimated travel time may be affected	Calculated shear wave velocities may be affected if large bender element penetrations are used in conjunction with small specimens. Higher transmitter frequencies will be needed to keep the wavelength down
Input wave form	Square, continuous sine or pulsed sine waves	Square wave pulses contain a broad spectrum of frequencies. Low frequencies place the receiver in the near field	Practice suggests single sine pulses produce acceptable traces, giving repeatable first break or peak-to-peak travel times, and permitting a more restricted and controllable input frequency
Input wave mode	P- or S-wave	In soft saturated soil P-waves travel at approx.1,450–1,550 m/s (the P-wave velocity of water), much faster than S-waves. In unsaturated soils P-waves travel only approx. 50% faster, and can obscure or be confused with S-waves	It is suggested that extender elements should be routinely used to warn of misinterpretation

TABLE 1. cont.

Issue	Brief description	Effect	Suggested standard
Input frequency	Low source frequencies produce long wavelengths	Long wavelengths place the receiver in the near field, affecting the received waveform and picked travel time	The receiver should be at least 2–3 wavelengths from the transmitter. It is suggested that, for routine triaxial testing, results are returned for a range of frequencies from about 2.5 to 12.5 kHz)
Data acquisition	Low voltage and temporal resolution reduce quality of captured traces	Picked arrival times become uncertain	In order that accuracy is not degraded by resolution. the sampling time interval should be less than 1st/100th of the travel time between transmitter and receiver. Voltage resolution should be better than 1st/100th of the amplitude of the received signal
Signal-to--noise ratio	Noise affects low-amplitude received signals	Picking of first arrival or peak times is subjective. A low signal-to-noise ratio increases scatter and tends to increase the estimated travel time	A study of some relatively noisy UK data suggests a minimum amplitude signal/noise ratio (S/N) as of 10. Leong et al. (2005) suggest a receiver S/N ratio of at least 4 dB
Method of determining travel time	First-break, peak-to-peak, cross-correlation, or phase/ /frequency relationship	Different processing methods lead to different travel times. With mixed frequencies pulse broadening may occur, owing to attenuation of the higher-frequency component, leading to increases in measured travel time when using peak-to-peak detection. Receiver first breaks may be hidden by noise, leading to increases in measured travel time when using this method	First-break and first-peak-to-first--peak travel time detection are favoured by Yamashita et al. (2007), who found significant differences in some cases where cross-correlation and phase/frequency methods were used. It is suggested that results from both the first break and the peak-to--peak methods be routinely reported

MATERIALS AND METHODS

The triaxial shear tests presented in this paper were performed in a cell with internal linking bars, which enables easy access to the sample at each stage of its preparation, and equipped with the bender elements at the top and the bottom platen. This type of cell also provides more reliable deformation characteristics in the consolidation and shearing stage of the test. The bender elements were inserted in the soil samples during the triaxial shear tests. The change in voltage applied to the transmitter causes it to bend and transmit a shear wave through the sample; the arrival of the shear wave at the other end of the sample is recorded by the receiver as a change in voltage (Viggiani 1995, Brignoli et al. 1996, Ka-
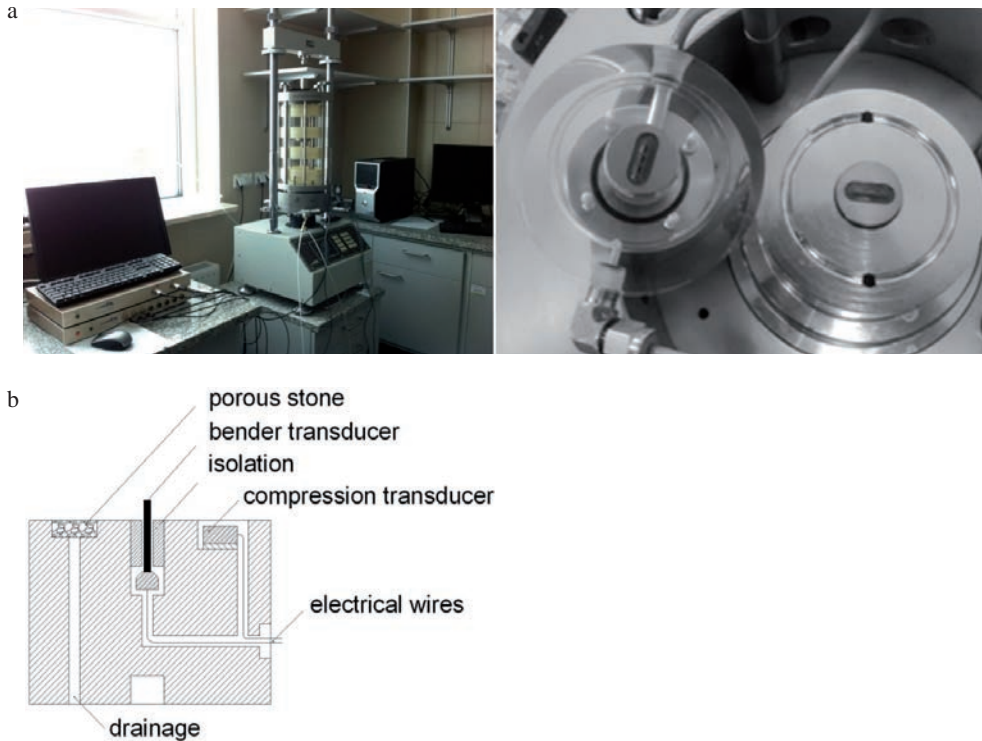
FIGURE 1. Research stand in the Laboratory – Water Center WULS-SGGW equipped with GDS Instruments devices (A division of Global Digital Systems Ltd); a – the bender elements at the top and the bottom platens of triaxial apparatus; b – schematic draw of triaxial base with bender element configuration (Brignoli et al. 1996)

waguchi et al. 2001). The bender element test setup is shown in Figure 1.

The methods of the interpretation of the arrival time of the shear wave can be classified into two main groups: the time-domain methods and the frequency-domain methods. In the time domain, the user visually determines the arrival time of the shear wave by examining the output and input signal voltages versus time. In the frequency domain, the input and output signals are transformed in the frequency domain (Vilhar and Jovicic 2009). Both groups of interpretation methods were focused on minimizing the influence of the dispersion and near--field effects.

The tested samples were taken from two test sites. The first one is a small village located to the south of Warsaw, at the experimental site of Warsaw University of Life Sciences. The results of the field tests (boreholes, CPT and DMT tests) and the laboratory tests showed that the stratigraphy consists of the Quaternary deposits including moraine clays and sandy clays (Markowska-Lech et al. 2016, Table 2). The free groundwater table is at a depth of about 2.0 m. The second location is Stegny, the southern district of Warsaw with

TABLE 2. Index properties of tested clays (Markowska-Lech et al. 2016)

Sample	Soil	Depth (m)	FC* (%)	w_n (%)	PI (%)	LI (-)	ρ (t/m^3)
1	sandy clay	0.9–4.0	11–15	9.7–16.7	17.6–23.9	–0.1-0.20	2.1
2	clay	4.0–12.0	4–11	11.9–15.9	2.99–20.4	0.05–0.20	2.05
3	clay	4.3–7.7	68–80	26–34	52.6–76.4	0.14–0.23	2.0–2.1
4	silty clay	7.7–8.9	30–34	19–25	39.3–55.6	0.04–0.22	2.0–2.4
5	clay	8.9–12	32–46	19–27	61.9–84.0	0–0.005	2.0–2.1

*Clay content (< 0.002 mm).

a stratigraphy including the Quaternary deposits developed as fine and medium density sand layers with the thickness of up to 4.5 m, underlain by the overconsolidated Pliocene clays. The clay beds feature a clear-layered structure with layers in different colours. The free groundwater table is at a depth of 3.2 m (Lech et al. 2009, Markowska-Lech and Bajda 2016).

The laboratory tests were carried out on 13 undisturbed clay and sandy clay samples and included: general index tests for classification and characterization of the clay, density, grain size distribution and measurement of shear wave velocity. The samples contained undisturbed natural Quaternary moraine clay and sandy clay (S1–S8) deposits and the lacustrine

TABLE 3. Index properties of soil samples tested in the triaxial tests

Sample	Depth (m)	FC* (%)	w_n (%)	ρ (t/m^3)	e_0 (-)
S1	1.2–1.7	11	12.9	2.17	0.392
S2	2.0–2.5	15	13.3	2.12	0.430
S3	4.0–4.2	12	12.2	2.10	0.430
S4	4.2–4.8	12	12.2	2.24	0.343
S5	5.0–5.5	13	10.6	2.30	0.286
S6	5.8–6.3	13	11.4	2.24	0.331
S7	6.5–7.0	4	11.2	2.24	0.331
S8	7.8–8.5	11	11.4	2.25	0.325
S9	6.5	68	21.8	2,08	0,595
S10	7.75	60	22.1	2,0	0,657
S11	8.5	29	20.4	1,84	0,784
S12	9.0	36	32.1	1,86	0,929
S13	9.95	63	27.9	1,90	0,833

*Clay content (< 0.002 mm).

deposits of the Pliocene clay (S9–S13), retrieved using a Shelby sampler from the depths between 1.2–7.8 m (S1–S8) and 6.5–9.95 m (S9–S13), respectively. The tested soil samples were characterized as follows: water content w_n from 10.6 to 32.1%, liquidity index (*LI*) from 26.5 to 88.1%, plastic limit *PL* from 9.9 to 32.2%, plasticity index (*PI*) from 14.8 to 60.6%, and clay content (*FC*) from 4 to 68%. In Table 3 the physical properties of all tested samples are summarized.

LABORATORY TESTS AND RESULTS

In this study, the triaxial shear tests were performed on 13 undisturbed clay samples in three stages: saturation (backpressure method), consolidation and shearing (strain-controlled mode at strain rate of 0.005 mm/min). The samples were consolidated in an isotropic stress condition. Shear wave velocity was measured at the end of each of saturation and consolidation stages during the triaxial shear tests. The single sine waves with frequencies of 1–10 kHz were used as an input signal. The shear wave velocity (V_s) was calculated from the ratio of the tip-to-tip distance (Viggiani and Atkinson 1995) between the transmitter and the receiver, using the following relationship:

$$V_s = h \, / \, t \tag{2}$$

where:
h – distance between the transmitter and the receiver geophones (the effective wave travel path through the sample);
t – travel time of seismic waves between the transmitter and the receiver.

The initial shear modulus was calculated from Equation (1). The initial arrival time of the shear wave to the receiver (R_d) can be affected by the near-field effect disturbances, described by the formula:

$$R_d = h \, / \, \lambda = (h \, f_{in}) \, / \, V_s \tag{3}$$

where:
h – effective wave travel length (m);
λ – wave length (m);
f_{in} – input signal frequency (Hz).

If the ratio of the distance to wavelength (R_d) is greater than 2, it has been perceived that the near-field effect can be ignored when the shear wave is measured. However, it can be seen that in the case of a medium with 5% material damping the arrival of the shear wave is marked by a smooth slope, not a sharp slope, even though R_d is greater than 4, while the shear wave presents a clear arrival with no damping. This is due to coupling of the shear wave and near-field wave. The initial arrival of the shear wave is located near the bump when R_d is 0.5 and moves in the direction of the first peak of the shear wave with an increase in R_d. Therefore, it is difficult to determine the travel time reliably from the first arrival of the shear wave. On the other hand, if the travel time is calculated using the time between the first peaks of the input and received waves, error in the travel time is less than 2% when R_d is greater than 2 (Youn et al. 2008).

Figures 2 and 3 show the traces obtained in bender element tests on sample S10 with different R_d values from 0.52 to 4.10 which correspond in this case
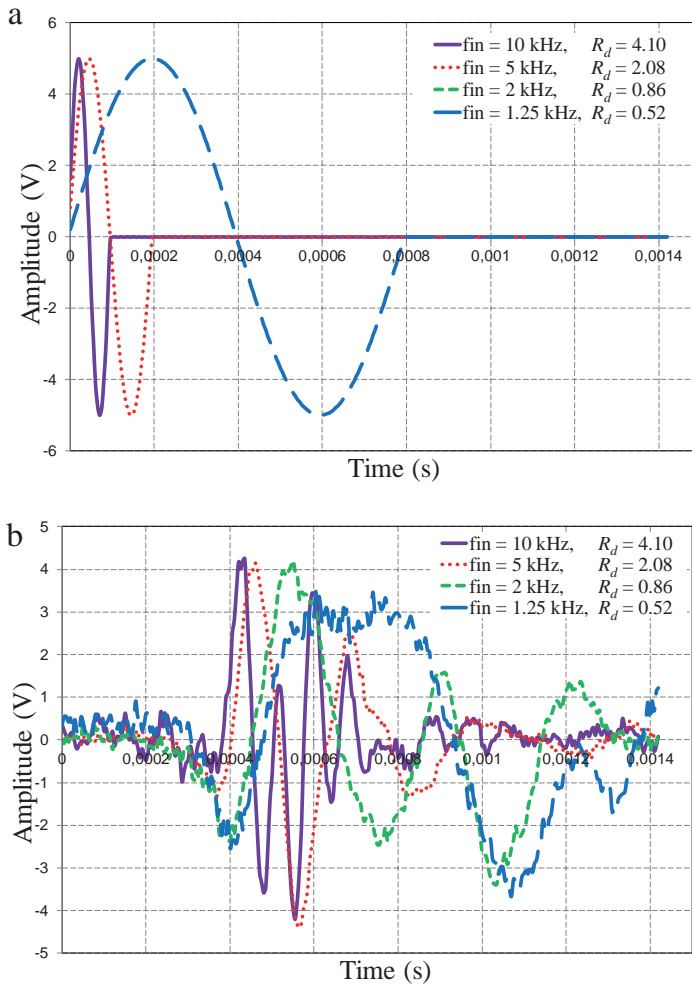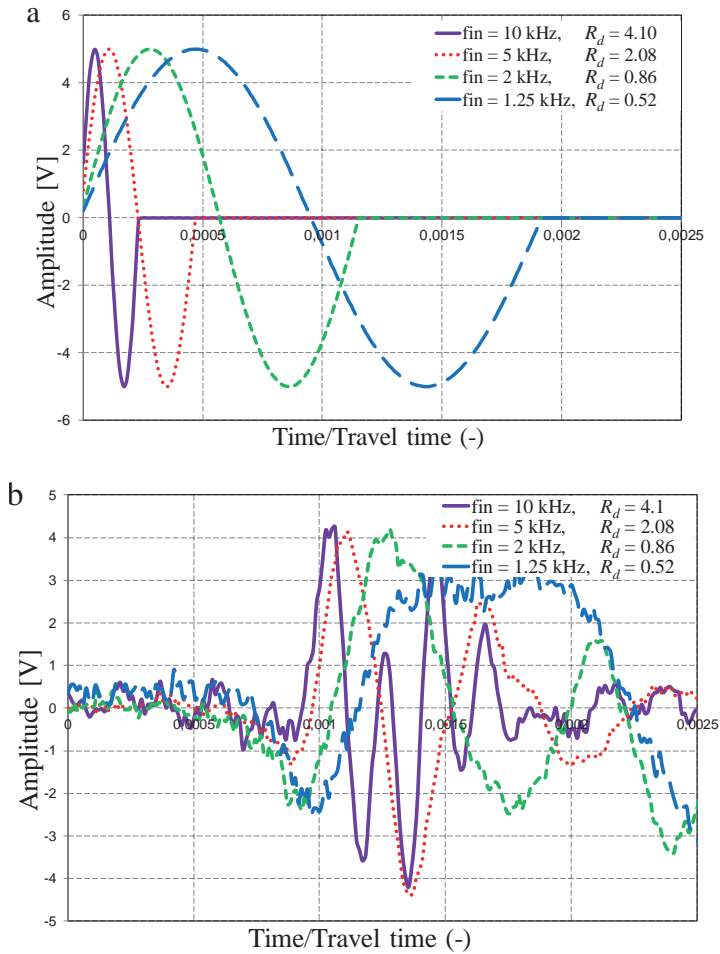
FIGURE 2. Example waveforms four signals with different wave lengths and values of R_d obtained in bender element tests on natural clays (sample S10; mean effective stress equal to 930 kPa; (a) transmitted signals, (b) received signals

to frequencies from 1.25 to 10 kHz, respectively. The time scale has been normalized with respect to the arrival time of the shear wave determined by visual peak-to-peak method. For low values of R_d there is an initial downward deflection of the trace before the shear wave arrives, representing the near-field effect. At higher R_d the near-field effect is much smaller, almost absent. In tested soil samples, the input signals with $R_d < 1$ do not usually produce a readable output. On the other hand, high frequency inputs did not always produce the best output; sometimes it was impossible to identify the arrival time.

Figure 4 presents the test results performed on sample S10 that show the

a

b

FIGURE 3. Example waveforms four signals with different wave lengths and values of R_d obtained in bender element tests on natural clays (sample S10, mean effective stress equal to 930 kPa); the time scale has been normalized with respect to the arrival time of the shear wave determined by peak-to-peak method; (a) transmitted signals, (b) received signals

influence of the transmitted signal frequency from 1.25 to 10 kHz on shear wave velocity (the arrival time was determined by the peak-to-peak method). The shear wave velocity increases with increasing of the mean effective stress for different frequencies of the input signal. The relationship between the shear wave velocity and the input signal frequency cannot be clearly determined: the highest values of the shear wave velocity were obtained for transmitted signal frequency of 10 kHz irrespective of the mean effective stress level, the lowest values of the shear wave velocity were obtained for input signal frequency of 1.25 kHz at mean effective stress of 155 kPa only and for transmitted signal
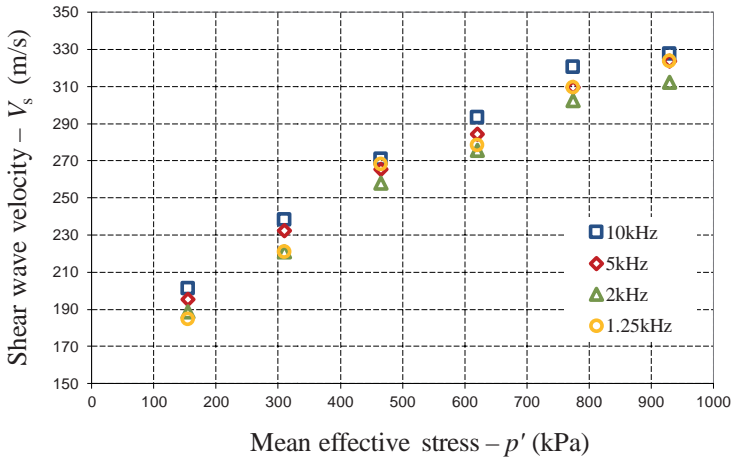
FIGURE 4. The influence of the transmitted signal frequency on shear wave velocity (peak-to-peak method; sample S10)

frequency of 2 kHz in others stress level. In the case of the mean effective stress of 310 kPa, the shear wave velocity equal 216 m/s for both lowest transmitted signal frequency: 1.25 and 2 kHz.

There are several different approaches in identifying the arrival time of the shear wave. The first one is by observing the transmitted and received wave signal and finding their difference as a propagation time in the soil specimen. Since this method uses a time base axis in order to identify the propagation's time, it is often called the time domain technique (*TD*). With this method, the arrival time of the shear wave is affected by the near-field-effect disturbances, the influence of the compression wave signals and other electric noises and reflections etc. It often makes the reading of arrival time quite difficult (Yamashita et al. 2007, Sas et al. 2015, Sas et al. 2016).

Viggiani and Atkinson (1995) compared different first arrivals of the received signal at different potential points. Point *A* is the first deflection;

point *B* is the first inflection (first bump maximum); point *C* is the first zero after inflection (zero crossing); and point *D* is the second inflection (Fig. 5).

These methods depend on a visual determination of the first major positive departure of the received signal from zero amplitude; they can only be used if the received signal is clear and remains flat before the first deflection. A better method than the visual picking of the first deflection point may be
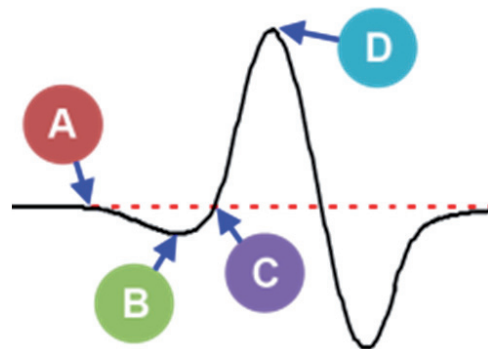

FIGURE 5. Potential arrival points (after Viggiani and Atkinson 1995)

the first major peak-to-peak method. It compared the time between the first two major peaks of the transmitted and the received signals. This method is not affected by the distortion of the received signal or by the near-field effects, but it requires good quality of the signals.

Another way is to calculate the arrival time on the basis of the time (time domain) or frequency (frequency domain) axis. The cross-correlation (*CC*) between the transmitted and the received wave is based on the presumption that the transmitted shear wave retains its wave shape, i.e. frequency even when it is passed into the soil. In this method, the *CC* of transmitted and the received wave is first evaluated and the position at the maximum amplitude is taken as the propagation time. However, there are times when frequencies of transmitted and received waves do not agree and the second peak or the next one at the received wave, rather than the first one, becomes larger in amplitude. Further-

more, as this method calculates arrival time using the time base axis, it is often said to be identical to the *TD*. The second method calculates the cross spectrum of the transmitted and the received waves producing the relations of the amplitude and phase angle with frequency axis. The arrival time is then calculated from the inclination of the phase spectrum. As it uses the frequency characteristics of input and output waves, it is often called the frequency domain technique (*FD*) (Yamashita et al. 2007). In both method, an experienced researcher with a proper knowledge how to interpret the correlated result is needed and there is a subjective aspect to this testing technique.

In Figure 6 and Table 4 the results of determination of the shear wave velocity from bender element test using different analysis method at different arrival points performed on the sample S10 at the mean effective stress of 930 kPa and the input signal frequency of 5 kHz are
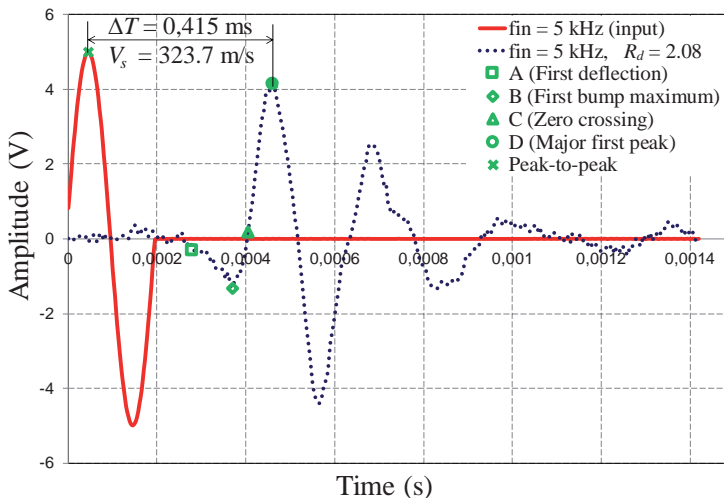

FIGURE 6. Different method of the travel time identification (sample S10, mean effective stress equal to 930 kPa, input signal frequency equal to 5 kHz)

TABLE 4. Determination of the shear wave velocity using different analysis method (sample S10, mean effective stress equal to 930 kPa, input signal frequency equal to 5 kHz; the arrival time in point *A*, *B*, *C*, *D* and *TD*, *FD* was read automatically by the *GDS* software)

Analysis method / arrival point	Travel time (ms)	Shear wave velocity (m/s)	ΔV_s (m/s)
A	0.280	479.8	156.1
B (first bump maximum)	0.370	363.1	39.4
C (zero crossing)	0.405	331.7	8.0
D	0.460	292.1	−31.7
Peak-to-peak	0.415	323.70	0
Cross-correlation (*TD*)	0.405	319.90	−3.9
Frequency domain (*FD*)	0.405	319.90	−3.9

shown. The tests results from different methods have been compared to the results from the visual picking method, which is so far the simplest, the most direct and the least time-consuming method.

In Figure 7 the relationship between the shear wave velocity and the mean effective stress from different analysis method i.e. peak-to-peak, the previous different arrival points namely point *A* (the first deflection), point *B* (the first inflection – first bump maximum), point *C* (the first zero after inflection – zero crossing) and point *D* (the second inflection) and *TD* (cross-correlation – time domain) and *FD* (frequency domain) obtained at the input signal frequency of 1.25, 2 and 5 kHz is presented. The results show the largest differences in the values of the shear wave velocity at the input signal frequency of 1.25 kHz (Fig. 7a), which indicate an uncertainty of the measurements at low input frequency, regardless of the

mean effective stress level during the next consolidation stage. The example of input signal frequency of 10 kHz (Fig.7d), show that the results obtained from point *B* and *C* method are irregularly distributed and the results from *A* method could not be determined; this indicates a significant disturbance of the received signal. The smallest differences in values of the shear wave velocity were obtained at the higher input frequency in peak-to-peak, point *C*, the *TD* and the *FD* methods independently from the mean effective stress level. Sometimes received signal makes it impossible to identify the arrival time of shear wave velocity.

In Figures 8–11 the laboratory test results for the bender element tests, namely the relationship between the shear wave velocity, mean effective stress and void ratio, are displayed. The shear wave velocity varies from 150 to 420 m/s for sample S1–S8 from the first test site and from 100 to 320 m/s
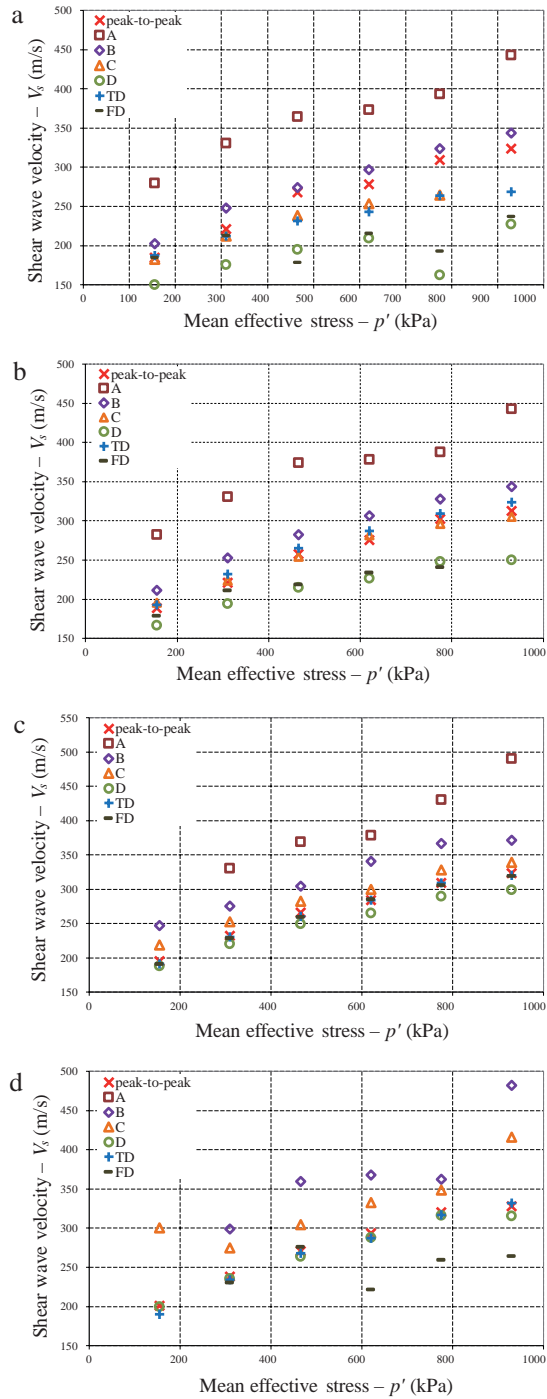
FIGURE 7. Shear wave velocity vs. mean effective stress from different analysis method: a – input signal frequency 1.25 kHz; b – input signal frequency 2 kHz; c – input signal frequency 5 kHz; d – input signal frequency 10 kHz (sample S10; the arrival time in point *A*, *B*, *C*, *D* and *TD*, *FD* was read automatically by the *GDS* software)

for sample S9–S13 from Stegny test site within the mean effective stress range between 15 and 1,000 kPa. An increase in the mean effective stress during the next consolidation stage decreases the void ratio and as a result increases the shear wave velocity. In Figure 10 a visible difference between the shear wave velocity for soils derived from the first (samples S1–S8) and the second (S9–S13) tests sites can be noticed due to different contents of clay fraction in the soil specimens. For the first group of the specimens the increase of shear wave velocity is faster and it achieves higher values than for the second group. The highest increase in the shear wave velocity is observed for sample S8 from the first test site and the lowest is observed for sample S12 from Stegny site. A similar relationship can be observed in Figures 12–14; the increase of the shear modulus at small strain is faster and it achieves higher values in the first group of soil speci-mens (S1–S8) in comparison with the second group. The shear modulus G_0 presented in Figures 12–14, calculated using the elastic theory from equation (1) reaches the values from about 50 to 400 MPa for deposits from the first test site and from 50 to 220 MPa for clays from Stegny site.

Virtually horizontal lines drown between the obtained data for individual specimens in Figures 8–14 indicate the changes in stress, which affect the shear wave velocity (and the shear modulus) to a lesser degree in high plasticity soil.

The values of the shear wave velocity and the shear modulus at small strain (G_0) obtained using bender elements techniques are lower than those obtained from the field tests (Markowska-Lech et al. 2016). To sum up, the soil stiffness values obtained in the field tests are expected to be higher than the values obtained from the laboratory tests due to the possible disturbance of the soil specimens.
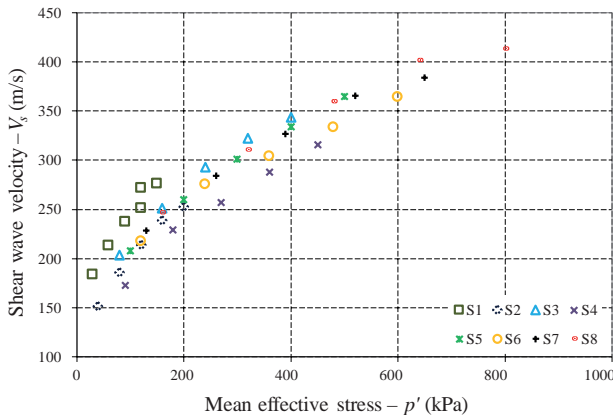

FIGURE 8. Shear wave velocity in clays vs. mean effective stress based on laboratory tests (S1–S8 samples)
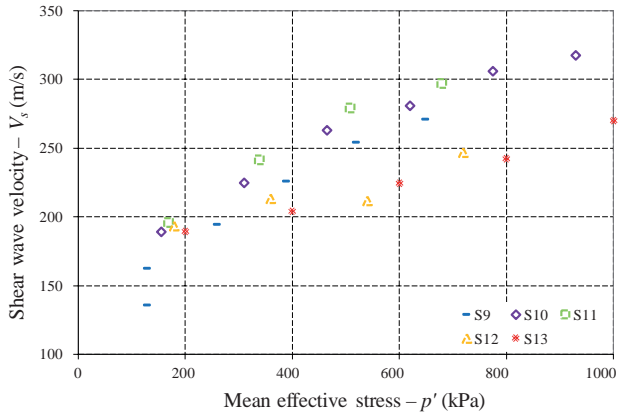
FIGURE 9. Shear wave velocity in clays vs. mean effective stress based on laboratory tests (S9–S13 samples)
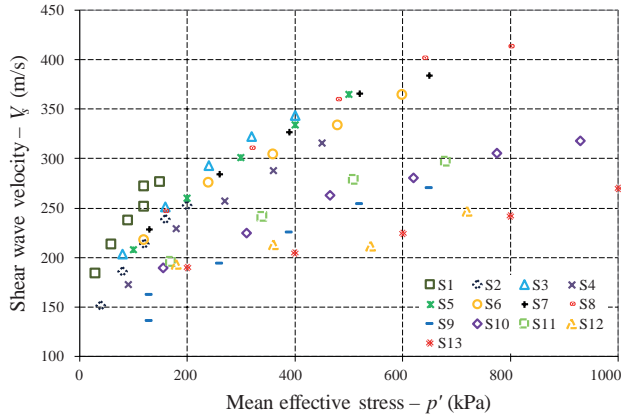

FIGURE 10. Shear wave velocity in clays vs. mean effective stress based on laboratory tests (S1–S13 samples)
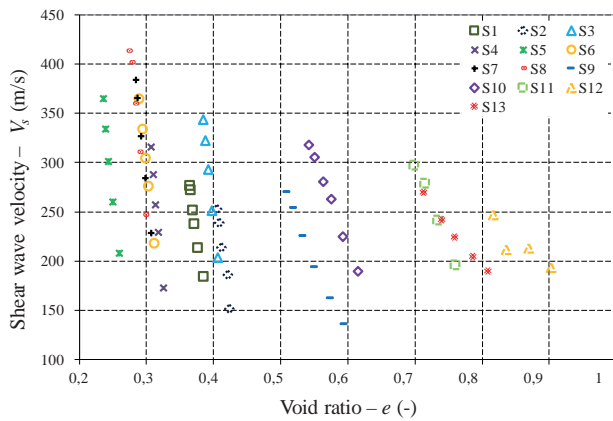

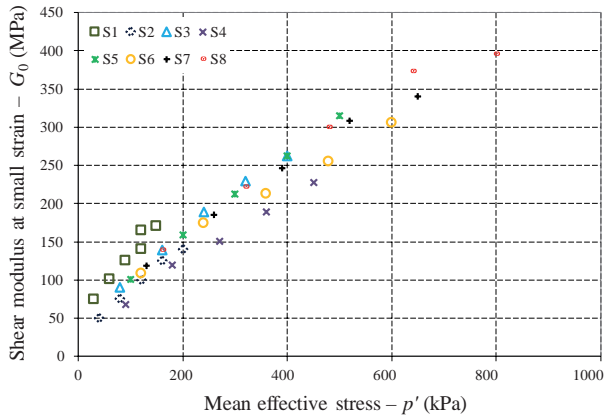FIGURE 11. Shear wave velocity in clays vs. void ratio based on laboratory tests (S1–S13 samples)

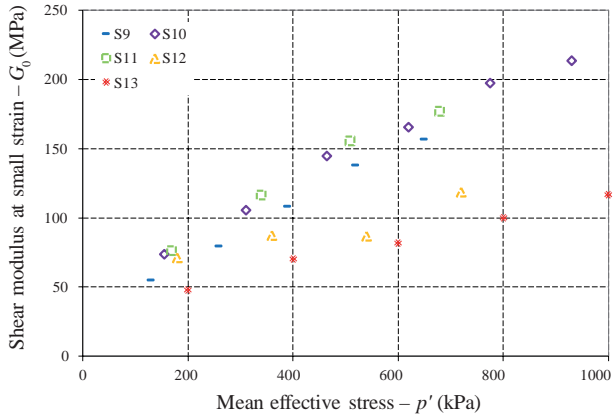FIGURE 12. Shear modulus for clays based on laboratory tests (S1–S8 samples)

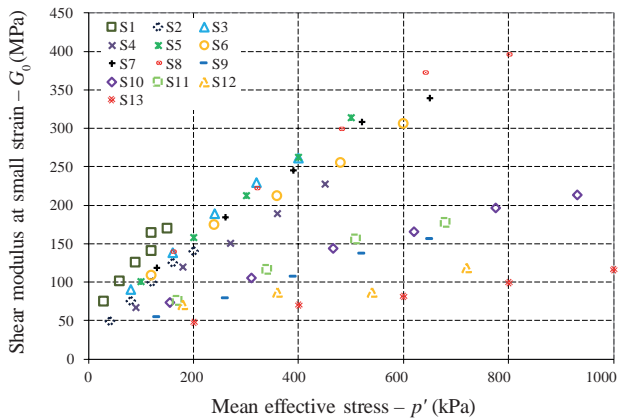FIGURE 13. Shear modulus for clays based on laboratory tests (S9– S13 samples)

FIGURE 14. Shear modulus for clays based on laboratory tests (S1–S13 samples)

CONCLUSIONS

The following conclusions can be drawn from presented experimental results:

− The input frequency range given by $R_d > 1$ readable output is likely, the upper range may be decided from the visibility of the received signal; in the tested specimens, higher input did not always produce the best signal.

− In every method for identification of the arrival time of the shear wave, an experienced researcher with a proper knowledge how to interpret the correlated result is necessary; there is a subjective aspect to this testing technique; there is available an automatic system for the travel time estimation process, but it still requires technician control.

− The mean effective stress and the void ratio significantly affect the shear wave velocity in the tested soils; there is a linear relationships between the mean effective stress and the shear wave velocity at a very small strain.

− Despite a high correlation between the shear wave velocity and the mean effective stress and the void ratio for tested soils, the investigation must be continued to establish the influence of stress history on the shear modulus, in particular in highly overconsolidated cohesive soils.

REFERENCES

ARULANTAN R., BOULANGER R.W., RIEMER M.F. 1998: Analysis of bender element tests. Geotech. Test. J. 21 (2): 120–131.

BRIGNOLI E., GOTTI M., STOKOE K.H. II 1996: Measurement of shear waves in laboratory specimens by means of piezoelectric transducers. ASTM Geotech. Test. J. 19 (4): 384–397.

CHEE-MING Ch. 2012: Variations of Shear Wave Arrival Time in Unconfined Soil Specimens Measured with Bender Elements. Geotech. Geol. Eng. 30: 461–468. DOI:10.1007/s10706-011-9480-3

CLAYTON C.R.I. 2011: Stiffness of small strain: research and practice. Géotechnique 61 (1): 5–37.

HARDIN B.O., BLACK W.L. 1968: Vibration modulus of normally consolidated clay. J. Soil Mech. Found. Div. ASCE 94 (2): 353–368.

JOVICIC V., COOP M.R., SIMIC M. 1996: Objective criteria for determining G_{max} from bender element tests. Géotechnique 46 (2): 357–362.

KAWAGUCHI T., MITACHI T., SHIBUYA S. 2001: Evaluation of shear wave travel time in laboratory bender element test. In: Proceedings of 15th International Conference on Soil Mechanics and Geotechnical Engineering, Istanbul, Vol. 1: 155–158.

LECH M., BAJDA M., MARKOWSKA-LECH K. 2009: The use of resistivity and seismic cone penetration tests for site characterization. Ann. Warsaw Univ. Life Sci. – SGGW. Land Reclam. 40 (1): 87–96.

LEE J-S., SANTAMARINA C. 2005: Bender elements: performance and signal interpretation. J. Geotech. Geoenviron. Eng. 131 (9): 1063–1071.

LEONG E.C., YEO S.H., RAHARDJO H. 2005: Measuring shear wave velocity using bender elements. Geotech. Test. J. 28 (5): 488–498. DOI: 10.1520/GTJ12196

LIPIŃSKI M.J., WDOWSKA M.W., JAROŃ J. 2017: Shear wave velocity for evaluation of state of cohesionless soils with fines. IOP Mat. Sci. Eng. 245, #032083. DOI: 10.1088/1757-899X/245/3/032083

LOPRESTI D.C.F., PALLARA O., JAMIOLKOWSKI M., CAVALLARO A. 1999: Anisotropy of small stiffness of undisturbed and reconstituted clays. In: R.J. Jardineet al. (Eds.), Pre-failure Deformation of Geomaterials. Balkema, Rotterdam: 3–10.

MARKOWSKA-LECH K., BAJDA M. 2016: Wyznaczanie modułu odkształcenia postaciowego G_0 w iłach [Estimation of shear modulus G_0 for clays]. Sci. Rev. Eng. Env. Sci. 71: 3–12.

MARKOWSKA-LECH K., SAS W., GABRYŚ K., BAJDA M., LECH M. 2016: Determination of the small strain stiffness of selected cohesive soils from Warsaw, Poland. In: 16th International Multidisciplinary Scientific Geoconference SGEM 2016, Albena, Book 1, Vol. 3: 77–84.

PELLI F., MINUTO D., ISETTA E., LOMBARDI G. 2004: Geotechnical characterization of an overconsolidated Pliocene clay by field and laboratory tests. In: Proceedings ISC-2 on Geotechnical and Geophysical Site Characterization. Millpress, Rotterdam: 1827–1834.

PN-EN ISO 14688:2006. Badania geotechniczne. Oznaczanie i klasyfikowanie gruntów [Geotechnical investigation and testing. Identification and classification of soil].

SAS W., GABRYŚ K., SZYMAŃSKI A. 2015: Effect of Time on Dynamic Shear Modulus of Selected Cohesive Soil of One Section of Express Way No. S2 in Warsaw. Acta Geoph. 63 (2): 398–413. DOI: 10.2478/s11600-014-0256-z

SAS W., GABRYŚ K., SOBÓL E., SZYMAŃSKA A. 2016: Dynamic Characterization of Cohesive Material Based on Wave Velocity Measurements. Appl. Sci. 6 (2): 49. DOI: 10.3390/app6020049

SCHNAID F. 2005: Geo-characterization and properties of natural soils by in situ tests. In: Proceedings of the 16th International Conference on Soil Mechanics and Geotechnical Engineering, Osaka. Millpress, Rotterdam: 3–45.

SCHNEIDER J.A., HOYOS L. Jr, MAYNE P., MACARI E.J., RIX G.J. 1999: Field and laboratory measurements of dynamic shear modulus of Piedmont residual soils. ASCE Geotechnical Special Publication 92: 12–25.

STOKOE K.H II, RATHJE E.M., AXTELL P.J. 2005: Development of an in situ method to measure the nonlinear shear modulus of soil. In: Proceedings of the 16th International Conference on Soil Mechanics and Geotechnical Engineering, Osaka. Millpress, Rotterdam: 751–754.

VIGGIANI G. 1995: Panelist discussion: Recent advances in the interpretation of bender element tests. In: Pre-failure Deformation of Geomaterials. Balkema, Rotterdam, Vol. 2: 1099–1104.

VIGGIANI G., ATKINSON J.H. 1995: Interpretation of bender element tests. Géotechnique 45 (1): 149–154.

VILHAR G., JOVICIC V. 2009: Measurement and interpretation of the small strain stiffness of Bostanj silty sand. Acta Geotech. Slov. 2: 57–75.

WOLSKI W., LIPINSKI M.J. 2006: Site characterization for geotechnical and environmental purposes. In: Proceedings of the 13th Danube-European Conference on Geotechnical Engineering, Ljubljana, Vol. 1: 129–150.

YAMASHITA S., FUJIWARA T., KAWAGUCHI T., MIKAMI T., NAKATA Y., SHIBUYA S. 2007: International parallel test on the measurement of G_{max} using bender elements. Retrieved form: http://www.jiban.or.jp/e/tc29/BE_Inter_PP_Test_en.pdf.

YOUN J-U., CHO O-W., KIM D-S. 2008: Measurement of small-strain shear modulus G_{max} of dry and saturated sands by bender element, resonant column, and

torsional shear tests. Can. Geotech. J. 45: 1426–1438. DOI: 10.1139/T08-069

ZENG X., NI B. 1999: Stress-induced anisotropic G_{max} of sands and its measurement. J. Geotech. Geoenviron. Eng. 125 (9). DOI: 10.1061/(ASCE)1090-0241(1999)125:9(741)

Streszczenie: *Sztywność gruntów spoistych w zakresie małych odkształceń z badań wykorzystujących piezoelementy typu bender*. Moduł odkształcenia postaciowego G_0 jest jednym z kluczowych parametrów w modelach sprężysto-plastycznych gruntu ze wzmocnieniem koniecznym w numerycznych analizach zagadnień współpracy konstrukcji z gruntem. Parametr ten może być wyznaczany na podstawie prędkości fal mechanicznych rozchodzących się w gruncie, mierzonych w badaniach laboratoryjnych i terenowych. Pomimo popularności tych badań problemem pozostaje interpretacja wyników pomiaru czasu przejścia fali przez próbkę gruntu, wynikająca z dużej liczby czynników wpływających na sztywność gruntu oraz na sam pomiar. Propozycje rozwiązań, które można znaleźć w literaturze, mogą służyć jedynie jako wskazówki do interpretacji konkretnego przypadku pomiaru. W artykule przedstawione zostały wyniki oraz interpretacja badań wykonanych na naturalnych gruntach spoistych z wykorzystaniem aparatu trójosiowego wyposażonego w piezoelementy typu bender.

Słowa kluczowe: sztywność gruntu w zakresie małych odkształceń, piezoelementy typu bender, grunty spoiste

Authors' address:

Mariusz Lech
Wydział Budownictwa i Inżynierii Środowiska
Szkoła Główna Gospodarstwa Wiejskiego
w Warszawie
ul. Nowoursynowska 159, 02-776 Warszawa
Poland
e-mail: mariusz_lech@sggw.pl